Epigenetic silencing of *HDAC1* by *miR-449a* upregulates *Runx2* and promotes osteoblast differentiation

TE LIU[1,2], LENGCHEN HOU[1], YANHUI ZHAO[3] and YONGYI HUANG[4]

[1]Shanghai Tenth People's Hospital, Medical School, Tongji University, Shanghai 200072;
[2]Shanghai Geriatric Institute of Chinese Medicine, Longhua Hospital, Shanghai University of Traditional Chinese Medicine, Shanghai 200031; [3]The Affiliated Stomatology Hospital of Tongji University, Shanghai 200072, P.R. China;
[4]Laboratoire PROTEE, Bâtiment R, Université du Sud Toulon-Var, 83957 La Garde Cedex, France

Abstract. Human-induced pluripotent (iPS) cells can be induced to differentiate into osteoblasts, but the process is inefficient and time-consuming. Previous studies indicated a close association between the expression of *Runx2* and osteoblast differentiation, and established that the transcriptional activation of the *Runx2* gene was closely associated with histone acetylation. microRNA-449a (*miR-449a*) represses *HDAC1* expression, thereby regulating histone acetylation. In the present study, whether the expression of *miR-449a* enhanced the generation of osteoblasts from human iPS cells was investigated. Introduction of *miR-449a* into human iPS cells resulted in the expression of osteoblast markers after only four days, compared to eight days for untransfected human iPS cells. Differentiation to osteoblasts was associated with a reduction in *HDAC1* expression, and higher levels of histone acetylation, particularly at the binding sites on the *Runx2* promoter in the human *miR-449a*-transfected iPS cells. Silencing of endogenous *HDAC1* expression by exogenous *miR-449a* therefore maintains histone acetylation status, stimulates *Runx2* gene expression and rapidly promotes osteoblast differentiation.

Introduction

Regenerative therapies for the treatment of cartilage injury have become an important focus for the field of stem cell therapy. Although pluripotent embryonic stem cells (ESCs) are the ideal seeds for cell therapy, there are ethical concerns on the use of donated, early human embryos and problems with tissue rejection in patients following transplantation (1-3). In order to overcome these issues, somatic cells have been reprogrammed to yield induced pluripotent stem (iPS) cells by introduction

of four essential transcription factors; *Oct3/4*, *Sox2*, *c-Myc* and *Klf4* (3-5). The iPS cells closely resemble ESCs; they can differentiate into cellular derivatives of all three germ layers and possess the capacity of unlimited replication (3,6). The iPS cells have the potential to provide an abundant cell source for tissue engineering, as well as generating patient-matched *in vitro* models to study genetic and environmental factors in cartilage repair and osteoarthritis (7). ESCs and iPS cells have been induced to differentiate into osteoblasts *in vitro*. Differentiation of ESCs towards the osteoblast lineage is enhanced by supplementing serum-containing media with ascorbic acid, β-glycerophosphate, dexamethasone and retinoic acid, or by co-culture with fetal murine osteoblasts (8). Recently, two studies have reported that mouse iPS cells could be induced to differentiate into osteoblasts *in vitro* (7,9). The latter study also demonstrated the potential use of mouse iPS cells in the repair of cartilage defects and in the generation of tissue models of cartilage that were matched to specific genetic backgrounds (7). Finally, it has been shown that human iPS cells can be cultured on microchannel polycaprolactone scaffolds prepared using a robotic dispensing technique, with osteogenesis promoted by the addition of exogenous osteogenic factors (3). However, despite the success in facilitating the differentiation of iPS cells or ESCs into osteoblasts *in vitro*, the process is inefficient and time-consuming, and this has hindered their development and therapeutic potential.

Mesenchymal stem cells can differentiate into mature and functional osteoblasts that produce extracellular matrix proteins and proteins that regulate matrix mineralization (10). *Runx2*, also known as Cbfa1/AmI3, is a runt domain family protein, which acts as an osteoblast-specific transactivator essential for osteoblast differentiation and bone formation (10-14). Zhang *et al* (11) showed that commitment of undifferentiated mesenchymal stem cells to an osteoprogenitor lineage was associated with the expression of *Runx2*, and *Runx2* protein levels were significantly upregulated in quiescence (G_0) or during proliferative arrest induced by serum deprivation or by contact inhibition of osteoblast cells (15). Notably, $Runx2^{-/-}$ mice show a complete lack of intramembranous and endochondral ossification, due to the maturation arrest of osteoblasts (10). *Runx2* regulates the expression of osteoblast-specific genes, including *ALP*, type I collagen and osteocalcin (10), and is

Correspondence to: Dr Te Liu, Shanghai Tenth People's Hospital, Medical School, Tongji University, 301 Middle Yanchang Road, Shanghai 200072, P.R. China
E-mail: teliu79@126.com

necessary throughout life to promote the differentiation of new osteoblasts during bone remodeling (10). The study by Hu *et al* (16) reported that histone deacetylation suppresses *Runx2* transcription. The study showed that several histone deacetylase (HDAC) inhibitors promoted osteoblast maturation and the expression of specific genes through upregulation of *Runx2* gene expression in bone marrow stem cells (16). This result clearly indicated that epigenetic regulation, particularly histone acetylation, was an important factor in regulating *Runx2* expression. Recently, epigenetic regulation has been considered as a significant mechanism for influencing stem cell differentiation. The unique patterns of DNA methylation and histone modifications have been found to play important roles in the induction of lineage-specific differentiation of bone marrow stem cells (16). HDAC enzymes alter the transcription of numerous genes involved in the control of proliferation, cell survival, differentiation and genetic stability (17). Previous studies revealed that a microRNA, *miR-449a*, interferes specifically with the expression of *HDAC1* (9,17-19). microRNAs (miRNAs) are small [~22 nucleotides (nt)] endogenous non-coding RNAs, which function at the post-transcriptional level by annealing to the 3'-untranslated region (3'-UTR) of target mRNAs to inhibit translation. They have emerged as key regulatory factors in development, organogenesis, apoptosis, cell proliferation, differentiation and tumorigenesis (1,2,9). Several groups have reported that *miR-449a* targets *HDAC1* and induces growth arrest of tumor cells derived from hepatocellular, prostate and lung carcinoma (17-19). In an independent study, Okamoto *et al* (9) demonstrated that six miRNAs, including *miR-10a/b*, *miR-19b*, *miR-9*, *miR-124a* and *miR-181a*, were crucial regulatory factors in the osteoblast differentiation of mouse iPS cells.

In view of this evidence, the present study attempted to clarify whether overexpression of *miR-449a* suppressed *HDAC1* expression, increased *Runx2* expression and stimulated the differentiation of human iPS cells into osteoblasts. Therefore, if successful this procedure may improve the efficiency of generating osteoblasts from human iPS cells *in vitro*, and provide a reliable source for cell therapy.

Materials and methods

Preparation of human amniotic epithelial cells (HuAECs). Human placentas were obtained with written and informed consent from pregnant females who were negative for human immunodeficiency virus-I, hepatitis B and hepatitis C. The study was recognized for the appropriate use of human amnion by the Institutional Ethics Committee. This study was approved (Permit THTJHE20130018) by the Medical Ethics Committee of Tongji University, in compliance with the Experimental Medical Regulations of the National Science and Technology Commission, China. Amnion membranes were mechanically peeled from the chorines of placentas obtained from females with an uncomplicated Cesarean section. The epithelial layers with the basement membrane attached were obtained and used to harvest HuAECs as previously described with some modification (1,20). Briefly, the membrane was placed in a 250-ml flask containing Dulbecco's modified Eagle's medium (DMEM) and cut with a razor to yield 0.5-1.0-cm^2 segments. The segments were

digested with 0.25% trypsin-EDTA at 37˚C for 45 min. The resulting cell suspension were seeded in a six-well plate in DMEM medium supplemented with 10% fetal calf serum (PAA, Pasching, Austria), penicillin (100 U/ml) and glutamine (0.3 mg/ml), and incubated in a humidified tissue culture incubator containing 5% CO_2 at 37˚C. The HuAECs grown to a density of ~100% were used as feeder layers for human iPS culture following Mitomycin C (Sigma-Aldrich, St. Louis, MO, USA) treatment.

Co-culture of human iPS cells with HuAECs. The human iPS cells were generated as previously described (1). iPS cultures were separated from the feeder cells by treatment of 0.125% trypsin-EDTA solution and plated onto, and co-cultured with, HuAECs. The cells were cultured in DMEM:F12 (1:1) medium supplemented with 15% KnockOut™ Serum Replacement, 1 mM sodium pyruvate, 2 mM L-glutamine, 0.1 mM non-essential amino acids, 0.1 mM β-mercaptoethanol and penicillin (25 U/ml)-streptomycin (925 mg/ml), and mixed, but without leukemia inhibitory factor (LIF). These cells were incubated in a humidified tissue culture incubator containing 5% CO_2 at 37˚C. All the cells had been cultured on the same feeder until the 5th passage prior to undergoing the ulterior experiments.

Recombinant lentivirus generation vector construction and cell transfection. All the steps of the recombinant lentivirus package were as previously described (2,17-21). The Lv2-*miR-449a* and Lv2-miR-mut lentivirus were constructed by Genepharma Corporation (Shanghai, China) and the methods of lentivirus transfected were according to the manufacturer's instructions. In brief, co-transfection of human iPS cells was conducted using 4x10^7 PFU/ml Lv2-*miR-449a* or Lv2-miR-mut lentivirus, respectively, according to the manufacturer's instructions. The iPS cells were seeded in a six-well plate and cultured in DMEM:F12 (1:1) medium supplemented with 15% KnockOut™ Serum Replacement, 1 mM sodium pyruvate, 2.0 mM L-glutamine, 0.1 mM non-essential amino acids, 0.1 mM β-mercaptoethanol and penicillin (25 U/ml)-streptomycin (925 mg/ml), and mixed, but without LIF. These cells were incubated in a humidified tissue culture incubator containing 5% CO_2 at 37˚C until 80% confluent.

Embryoid body (EB) formation and induction of differentiation into the osteoblasts-like cells. All the steps were as previously described (3,6-9,16). Briefly, for EB formation the iPS cells were dissociated with 0.125% trypsin-EDTA solution and suspended onto Petri dishes with DMEM:F12 (1:1) medium supplemented with 15% KnockOut™ Serum Replacement, 1 mM sodium pyruvate, 2 mM L-glutamine, 0.1 mM non-essential amino acids, 0.1 mM β-mercaptoethanol, penicillin (25 U/ml)-streptomycin (925 mg/ml), and mixed, but without LIF for 6 days. Subsequently, to induce EB cell differentiation, day 6 EB cells were cultured in induced cell-conditioned medium (DMEM: F12 (1:1) supplemented with 1% KnockOut™ Serum Replacement, 1 mM sodium pyruvate, 2 mM L-glutamine, 0.1 mM non-essential amino acids, penicillin (25 U/ml)-streptomycin (925 mg/ml), 10 mg/ml insulin, 10 ng/ml human epidermal growth factor, 10 ng/ml human basic fibroblast growth factor, 50 mg/ml ascorbic acid, 50 mM β-glycerophosphate, 1 mM dexamethasone, 1 mM all-trans-retinoic acid and 100 ng/ml

human recombinant BMP-4, mixed and incubated in a humidified tissue culture incubator containing 5% CO_2 at 37°C for 12 days until differentiated completely.

RNA extraction and analysis by reverse transcription-quantitative PCR (RT-qPCR). Total RNA was isolated with Trizol reagent (Invitrogen Life Technologies Corporation, Grand Island, NY, USA), according to the manufacturer's instructions (21). Briefly, cells ($3x10^8$/ml) were collected and 0.8 ml Trizol reagent was added. After incubating the sample for 5 min, 0.2 ml chloroform was added and the tubes were agitated vigorously and incubated for 2 min. The samples were centrifuged at 17,000 x g for 15 min at 4°C. Subsequently, the aqueous phases were transferred to clean tubes, and 0.4 ml isopropanol was added and mixed. Following another centrifugation, the total RNA was collected. The RNA samples were treated with DNase I (Sigma-Aldrich), quantified by a regular UV spectrophotometer and reverse-transcribed into cDNA with the ReverTra Ace-α First Strand cDNA Synthesis kit [Toyobo (Shanghai) Biotech Co., Ltd., Shanghai, China]. qPCR was conducted with a RealPlex4 real-time PCR detection system from Eppendorf (Hamburg, Germany), with the SyBR Green RealTime PCR Master mix [Toyobo (Shanghai) Biotech Co., Ltd.] as the detection dye. qPCR amplification was performed over 40 cycles with denaturation at 95°C for 15 sec and annealing at 58°C for 45 sec. Target cDNA was quantified with the relative quantification method. A comparative threshold cycle (Ct) was used to determine the gene expression relative to a control (calibrator), and steady-state mRNA levels are reported as an n-fold difference relative to the calibrator. For each sample, the marker gene Ct values were normalized with the formula: $\Delta Ct = Ct\_genes - Ct\_18S\ RNA$. To determine relative expression levels, the following formula was used: $\Delta\Delta Ct = \Delta Ct\_all\_groups - \Delta Ct\_control\_group$. The values used to plot relative expressions of genes were calculated with the expression as $2^{-\Delta\Delta Ct}$. The mRNA levels were calibrated on the basis of *18S rRNA* levels. The cDNA of each gene was amplified with primers as described in Table I.

Luciferase reporter gene assay. All the steps of the luciferase report assay were as previously described (2,20-22). NIH-3T3 cells were seeded at $3x10^4$/well in 48-well plates and co-transfected with 400 ng Lv2-*miR-449a* or Lv2-miR-mut vectors, 20 ng pGL3-HDAC1-3UTR-WT or pGL3-HDAC1-3UTR-Mut, and pGL-TK (Promega, Madison, WI, USA) using the Lipofectamine 2000 reagent according to the manufacturer's instructions. After 48 h transfection, luciferase activity was measured using the dual-luciferase reporter assay system (Promega) according to the manufacturer's instructions. The results were expressed as relative luciferase activity (Firely LUC/Renilla LUC).

RNA extraction and northern blotting analysis. All the steps of northern blotting were as previously described (2,20-22). For all groups, 20 μg of good quality total RNA was analyzed on a 7.5 M urea 12% polyacrylamide denaturing gel and transferred to a Hybond N+ nylon membrane (Amersham, Freiburg, Germany) with electrotransfer. The membranes were crosslinked using UV light for 30 sec at 1200 mJ/cm². Hybridization was performed with the *miR-17-3p* antisense starfire probe, 5'-ACCAGCTAACAATACACTGCCA-3';

Table I. RT-qPCR primers used in the study.

Gene name	RT-qPCR primers (5'→3')
HDAC1	F: TATTATGGACAAGGCCACCC
	R: CATCTCCTCAGCATTGGCTT
Runx2	F: ACAGTAGATGGACCTCGGGA
	R: ATACTGGGATGAGGAATGCG
Bmp4	F: TGAGCCTTTCCAGCAAGTTT
	R: GCATTCGGTTACCAGGAATC
Osterix	F: CTCAGCTCTCTCCATCTGCC
	R: GGGACTGGAGCCATAGTGAA
Osteopontin	F: GTGATTTGCTTTTGCCTCCT
	R: GCCACAGCATCTGGGTATTT
Osteocalcin	F: CTCACACTCCTCGCCCTATT
	R: TTGGACACAAAGGCTGCAC
18S rRNA	F: CAGCCACCCGAGATTGAGCA
	R: TAGTAGCGACGGGCGGTGTG

RT-qPCR, quantitative reverse transcription-polymerase chain reaction.

to detect the 22-nt *miR-17-3p* fragments according to the manufacturer's instructions. Following washing, the membranes were exposed for 20-40 h to Kodak XAR-5 films (Sigma-Aldrich). As a positive control, all the membranes were hybridized with a human *U6* snRNA probe, 5'-GCAGGG GCCATGCTAATCTTCTCTGTATCG-3'. Exposure times for the *U6* control probe varied between 15 and 30 min.

Western blot analysis. All group cells were seeded at $3x10^6$/ well in 6-well plates and cultured until 85%, which were lysed using a 2x loading lysis buffer [50 mM Tris-HCl (pH 6.8), 2% sodium dodecyl sulfate, 10% β-mercaptoethanol, 10% glycerol and 0.002% bromophenol blue]. The total cellular proteins from the cultured cells was subjected to 12% SDS-PAGE and transferred onto hybrid-PVDF membranes (Millipore, Bedford, MA, USA). Following blocking with 5% (w/v) skimmed dried milk in Tris-buffered saline containing Tween-20 [TBST; 25 mM Tris/HCl (pH 8.0), 125 mM NaCl and 0.05% Tween-20], the PVDF membranes were washed four times (15 min each) with TBST at room temperature and incubated with antibody dilution solution (Beyotime Institute of Biotechnology, Jiangsu, China) to dilute the following primary antibodies: Rabbit anti-human osterix polyclonal antibody (sc-133871), rabbit anti-human osteocalcin polyclonal antibody (sc-30044), rabbit anti-human osteopontin polyclonal antibody (sc-20788; all 1:1000; Santa Cruz Biotechnology, Inc., Santa Cruz, CA, USA), rabbit anti-human HDAC1 polyclonal antibody (no. 2062), rabbit anti-human *RUNX2* polyclonal antibody (no. 8486), rabbit anti-human BMP4 polyclonal antibody (no. 4680), rabbit anti-human H3K27Me3 polyclonal antibody (no. 9733), rabbit anti-human H3Ac polyclonal antibody (no. 7627) and rabbit anti-human GAPDH polyclonal antibody (no. 5174; all 1:1000; Cell Signaling Technology, MA, USA). Following extensive washing, membranes were incubated with horseradish peroxidase (HRP)-conjugated

goat anti-rabbit immunoglobulin G (IgG) secondary antibody (sc-2768; 1:1000; Santa Cruz Biotechnology, Inc.) for 1 h. Following washing four times (15 min each) with TBST at room temperature, the immunoreactivity was visualized by enhanced chemiluminescence (ECL) using the ECL kit from Perkin-Elmer Life Science (Norwalk, CT, USA). Subsequently, the chemisluminescent signals were detected by using a chemiluminescence detection system (GE Typhoon 9400; GE Healthcare, Shanghai, China).

ELISA assay. The alkaline phosphatase (ALP) ELISA kit (Hermes Criterion Biotechnology, Vancouver, BC, Canada) was used according to the manufacturer's instructions (16,23) to determine the level of ALP in cells. Briefly, all the cells were harvested and dissociated in 0.1 M Tris (pH 7.4) containing 1% Triton X-100 and 5 mM $MgCl_2$ by sonication. ALP concentration was measured and the data were normalized against the protein concentration and expressed as nanogram of ALP per milligram of total protein. All the samples were added to anti-ALP antibody precoated microtest wells and incubated for 60 min. Three washes were performed and the HRP-conjugated detection antibodies were added followed by the substrate solution. The absorbance was determined at a wavelength of 450 nm using the enzyme-linked immunosorbent assay reader (Model 680; Bio-Rad, Hercules, CA, USA).

Hematoxylin and eosin (H&E) staining. The histopathological analysis of each group was stained with H&E staining. Briefly, all fresh tissues were washed 3 times with PBS and fixed with 4% paraformaldehyde (Sigma-Aldrich) for 30 min, dehydrated through a graded series of ethanol, vitrified in xylene, and embedded in paraffin. Next, serial 6-μm-thick sections were cut, and stained with H&E.

Alkaline phosphatase-positive cell staining. All the steps were as previously described (6). Briefly, all the cells were washed twice with 0.01 M phosphate-buffered saline (PBS) and fixed in 4% paraformaldehyde for 20 min. Subsequent to fixing, the cells were rinsed with PBS twice, and PBS was replaced with 1 ml of the staining solution [Naphthol AS-MX phosphate (0.1 mg/ml) and fast blue BB salt (0.6 mg/ml)] dissolved in Tris-HCl buffer [0.1 M (pH 8.8)] containing N,N-dimethylformamide (0.5%) and $MgCl_2$ (2 mM) and the cells were incubated at 37°C for 60 min until the ALP-positive cells stained deep blue. The staining reaction was stopped by PBS solution. Digital images were captured with the Olympus IX71 microscope (Olympus Optical Co., Ltd., Tokyo, Japan).

Alizarin red histochemical staining. All the steps were as previously described (3,6-9,16). Briefly, cell culture plates were fixed in 4% paraformaldehyde for 20 min, washed in 0.01 M PBS and stained for 10 min with a 1% solution of Alizarin Red (Sigma-Aldrich). The plates were washed in running tap water and left to air dry. Manual counts of bone nodule colonies identified by Alizarin Red were subsequently performed.

Von Kossa assay for calcium determine. All the steps were as previously described (14). Briefly, cell culture plates were fixed with 95% ethanol for 20 min, and washed in distilled water. Subsequently, the cells were covered with a 1.0% $AgNO_3$ solution and maintained for 60 min under UV light until the calcium turned black. Following this, a 5.0% NaS_2O_3 solution was added for 2 min, and plates were washed in running tap water and left to air dry. Digital images were captured with the Olympus IX71 microscope.

Co-immunoprecipitation assay. All group cells were seeded at $3x10^5$/well in 6-well plates and cultured until 85% confluent (24). The cells were lysed (500 μl per plate) in a modified cell lysis buffer for western blotting and immunoprecipitation [20 mM Tris (pH 7.5), 150 mM NaCl, 1% Triton X-100, 1 mM EDTA, sodium pyrophosphate, β-glycerophosphate, Na_3VO_4 and leupeptin] (Beyotime institute of Biotechnology). Subsequent to lysis, each sample was centrifuged to remove the insoluble debris from the lysate and preincubated with 20 μg protein A agarose beads (Beyotime Institute of Biotechnology) by agitating for 30 min at 4°C, followed by centrifugation and transfer to a fresh 1.5-ml tube. The rabbit anti-human histone H3 polyclonal antibody (Cell Signaling Technology) was incubated for 90 min before re-addition of 20 μg protein A agarose beads to capture the immune complexes. The pelleted beads were washed three times with 500 μl cell lysis buffer, dissolved in 4x SDS-PAGE samples loading buffer and heated for 10 min at 95°C.

Chromatin immunoprecipitation (ChIP) assays. ChIP experiments were carried out using the anti-acetylated histone H3 antibody (Cell Signaling Technology), anti-trimethylated H3-K27 antibody (Cell Signaling Technology) and normal rabbit IgG (Upstate Biotechnology, Lake Placid, NY, USA) as a negative control. In brief, all the steps were performed as previously described (1,12,16). The cells were fixed by 1% formaldehyde for 30 min at 37°C and were quenched by 125 mM glycine for 10 min at room temperature to form DNA-protein cross-links. The samples were sonicated on ice until chromatin fragments became 200-1000 basepairs in size and incubated with antibodies at 4°C overnight. The PCR amplification was performed under the following conditions: 33 cycles of denaturation at 95°C for 30 sec, annealing at 55°C for 30 sec and extension at 72°C for 30 sec.

Statistical analysis. Each experiment was performed as least three times, and data are shown as the mean ± standard error where applicable. The differences were evaluated with Student's *t*-tests. A P-value of <0.05 was considered to indicate a statistically significant difference.

Results

miR-449a binding sites in the 3'-untranslated region (3'-UTR) of HDAC1 mRNA. The sequences of the *miR-449a* precursor, mature miRNA and the proposed target gene, *HDAC1*, were analyzed in multiple species using online research tools and the miRBase database (http://www.mirbase.org). In the present study, the potential human *miR-449a* target residues in the human *HDAC1* 3'-UTR were focused on, and seven consecutive putative miRNA target residues were identified that are conserved across species (Fig. 1). A luciferase activity assay was used to identify whether mature *miR-449a* binds to this site within the *HDAC1* mRNA 3'-UTR and regulates its expression. The luciferase activity of the *HDAC1* 3'-UTR
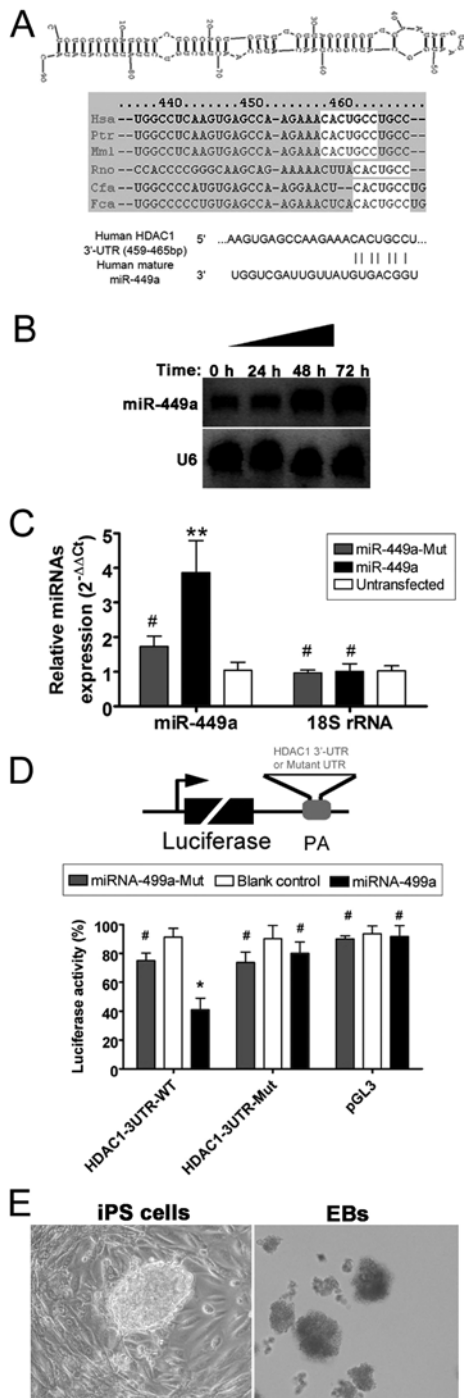
Figure 1. Secondary structure of *miR-449a* and expression levels in human-induced pluripotent (iPS) cells. (A) Typical secondary structure of human *miR-449a* precursor microRNA, containing stem-loop and hairpin structures. The potential binding site is located in an unstable region with a multi-branching loop-like RNA structure. The mature *miR-449a* is 100% identical across species. Sequences of human *miR-449a* and the human *HDAC1* 3'-untranslated region (UTR) (459-465 basepairs), showing the complementary bases. (B) Northern blot showing a strong hybridization signal corresponding to *miR-449a* in iPS cells following transfection. *U6* RNA was used as a loading control. (C) Reverse transcription-quantitative polymerase chain reaction showed an increase in the expression level of *miR-449a* in transfected iPS cells, compared to cells transfected with mutant *miR-449a* or untransfected cells (**P<0.01, vs. untransfected group; $^{\#}$P>0.05, vs. untransfected group; n=3). (D) The effect of *miR-449a* expression on *HDAC1* luciferase activity. Wild-type (WT) reporter or mutated control (Mut) luciferase plasmids were transfected into NIH-3T3 cells with lentivirus expressing *miR-449a*-WT or -mut. The luciferase activity of the *HDAC1* 3'-UTR construct was inhibited by *miR-449a*-WT (*P<0.05, vs. blank control; $^{\#}$P>0.05, vs. blank control; n=3). (E) Morphology of iPS cells and embryoid bodies (EBs). Magnification, x200.

was significantly inhibited by wild-type m*iR-449a* (Fig. 1), suggesting that *miR-449a* interacts with *HDAC1*. Mutation of either the *HDAC1* 3'-UTR construct or *miR-449a* to disrupt the potential interaction yielded results similar to the pGL3 control, indicating that the binding was specific. Detection of *miR-449a* miRNA by northern blotting and RT-qPCR confirmed that *miR-449a* expression was significantly increased 48-72 h following transfection of human iPS cells (Fig. 1).

miR-449a-transfected iPS cells efficiently differentiate into osteoblasts. Human iPS cells were transfected with a wild-type *miR-449a*, a mutant *miR-449a* or were untransfected. Subsequent to the formation of EB, differentiation was induced in the three groups of cells and examined over 12 days. The *miR-449a*-transfected iPS cells were the first to show the morphology of osteoblasts only four days after induction of differentiation; a proportion of the cell population showed quadrilateral or dwarf columnar morphology, and a honeycomb arrangement and neat rules, which was not evident in the other groups at that time (Fig. 2). Furthermore, at the early time-points there were more positively-stained cells in the *miR-449a*-transfected iPS cells compared to the *miR*-mut-transfected iPS cells or the untransfected group by several different assays (including the Von Kossa assay, Fig. 2B; Alizarin red staining, Fig. 2C; and staining for ALP, Fig. 2D). These experiments indicated that although osteoblasts were present in all three groups 12 days after induction of differentiation, they were already detectable after only four days in iPS cells transfected with *miR-449a*.

miR-449a-transfected iPS cells significantly express osteoblast markers upon differentiation. ELISA assay, RT-qPCR and western blotting were used to quantify the increase in expression of various markers. The concentration of ALP was increased in all cells in a time-dependent manner. However, the amount of ALP in *miR-449a*-transfected iPS cells was significantly higher at all time-points after the induction of differentiation compared to the other two groups (Fig. 3). The mRNA levels of several important cell markers were analyzed in each group by RT-qPCR, and the relative mRNA levels were normalized to *18S rRNA*, which served as an internal control. The results showed that osteopontin, osteocalcin, *BMP4*, osterix and *Runx2* were expressed at significantly higher levels in the *miR-449a*-transfected iPS group compared to the *miR*-mut-transfected iPS or untransfected groups at each time-point following induction of differentiation (Fig. 3). However, *HDAC1* was expressed at significantly lower levels in the *miR-449a*-transfected iPS group compared to the *miR*-mut-transfected iPS or untransfected group. The results of the RT-qPCR assays were confirmed by western blotting (Fig. 3), which revealed that the levels of osteocalcin, osterix and Runx2 were all higher in the *miR-449a*-transfected group, compared to the two control groups, whereas the levels of HDAC1 expression were lower in the *miR-449a*-transfected iPS group.

miR-449a improves the transcriptional activity of Runx2 via chromatin re-configuration. ChIP assays showed the acetylation and trimethylation levels of histone H3 in the *Runx2* promoter were similar in all three groups prior to differentiation. However, only four days after induction of differentiation, the acetylation levels of histone H3 (H3Ac) in the *Runx2*
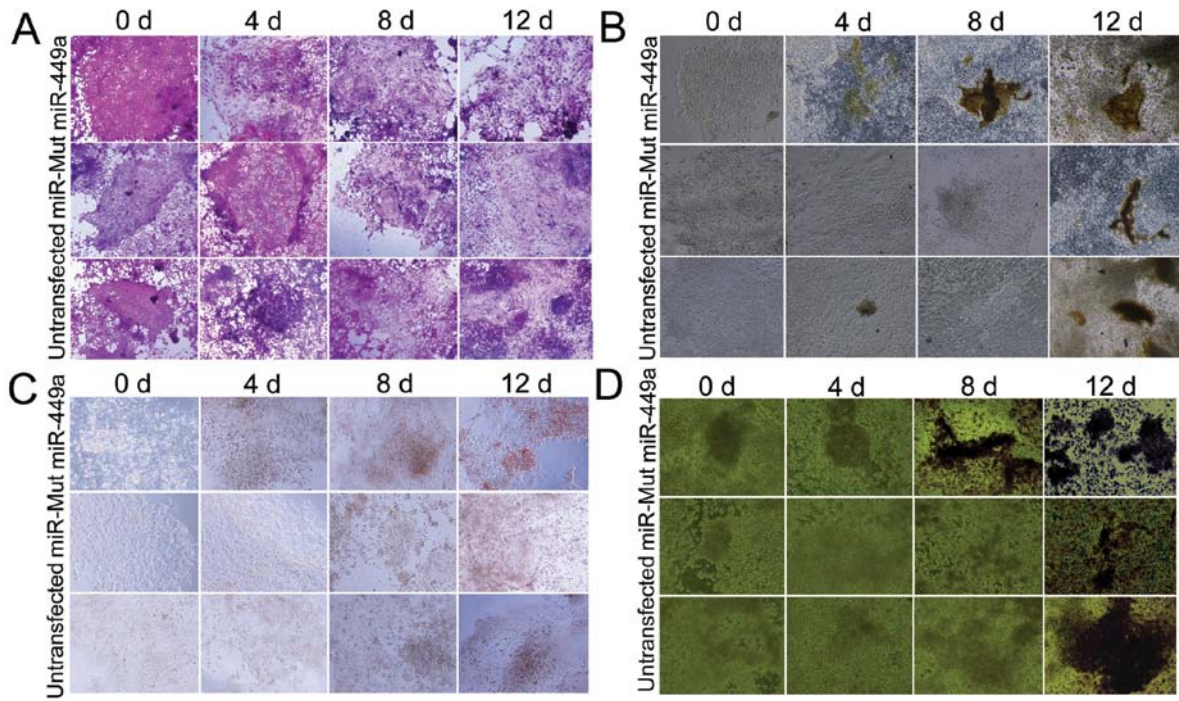
Figure 2. Immunohistochemical staining to confirm osteoblast differentiation. (A) Hemotoxylin and eosin staining indicated that *miR-449a*-transfected human-induced pluripotent (iPS) cells were the first to show osteoblast morphology on day four following the induction of differentiation. The (B) Von Kossa assay, (C) Alizarin red staining and (D) alkaline phosphatase (ALP)-positive cell staining indicated a much greater staining in *miR-449a*-transfected iPS cells compared to the *miR-mut*-transfected iPS cells or untransfected group, and at an earlier time-point. Magnification, x200. d, day.
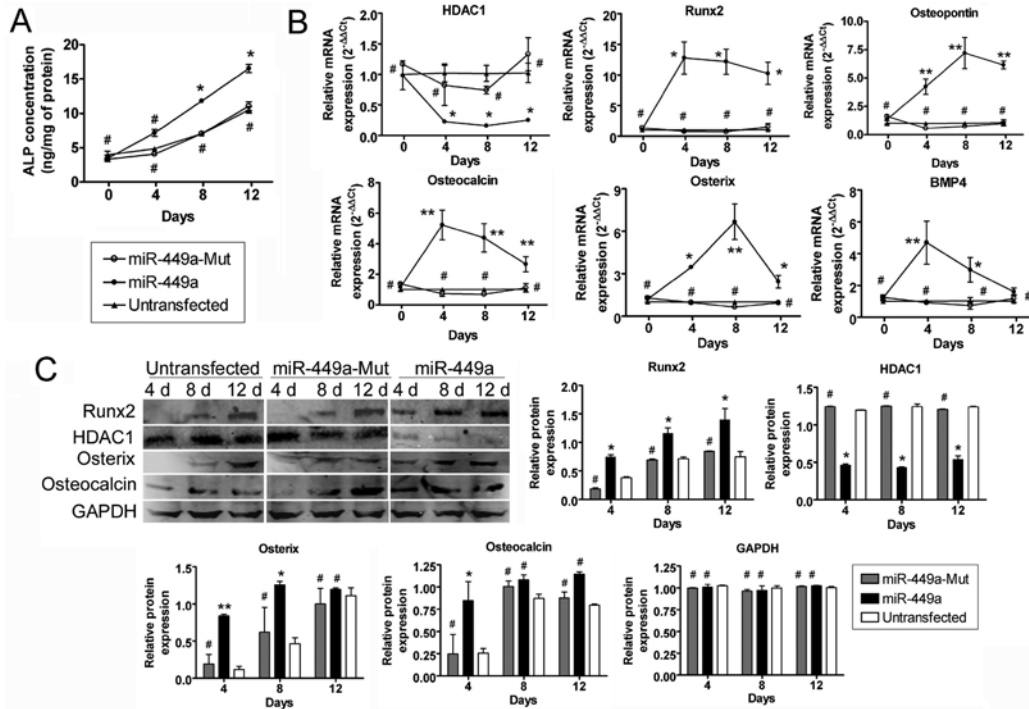

Figure 3. Osteoblast markers expression was assayed by the ELISA assay, reverse transcription-quantitative polymerase chain reaction (RT-qPCR) and western blotting. (A) The concentration of alkaline phosphatase (ALP) at each time-point after induction of differentiation was investigated by the ELISA assay. The results indicated that the rate of increase in ALP was significantly higher in the *miR-449a*-transfected human-induced pluripotent (iPS) cells compared to the other two groups. *$P<0.05$, vs. untransfected group; #$P>0.05$, vs. untransfected group; $n=3$. (B) RT-qPCR was used to compare the transcriptional levels of several important cell markers, including osteoblast markers and associated transcription factors following the induction of iPS cell differentiation. Relative mRNA expression was normalized to *18S* rRNA, which served as an internal control. The results showed that osteopontin, osteocalcin, *BMP4*, osterix and *Runx2* were expressed at significantly higher levels in the *miR-449a*-transfected iPS group compared to the other two groups at each time-point after induction of differentiation. However, *HDAC1* was expressed at significantly lower levels in the *miR-449a*-transfected iPS group compared to the other groups. **$P<0.01$, vs. untransfected group; *$P<0.05$, vs. untransfected group; #$P>0.05$, vs. untransfected group; $n=3$. (C) Western blotting revealed that the levels of osteocalcin, osterix and *Runx2* were significantly higher in the *miR-449a*-transfected cells compared to the *miR-mut*-transfected or untransfected groups. By contrast, the levels of *HDAC1* were much lower in the *miR-449a*-transfected iPS group compared to the *miR-mut*-transfected or untransfected group. **$P<0.01$, vs. untransfected group; *$P<0.05$, vs. untransfected group; #$P>0.05$, vs. untransfected group; $n=3$. d, day.
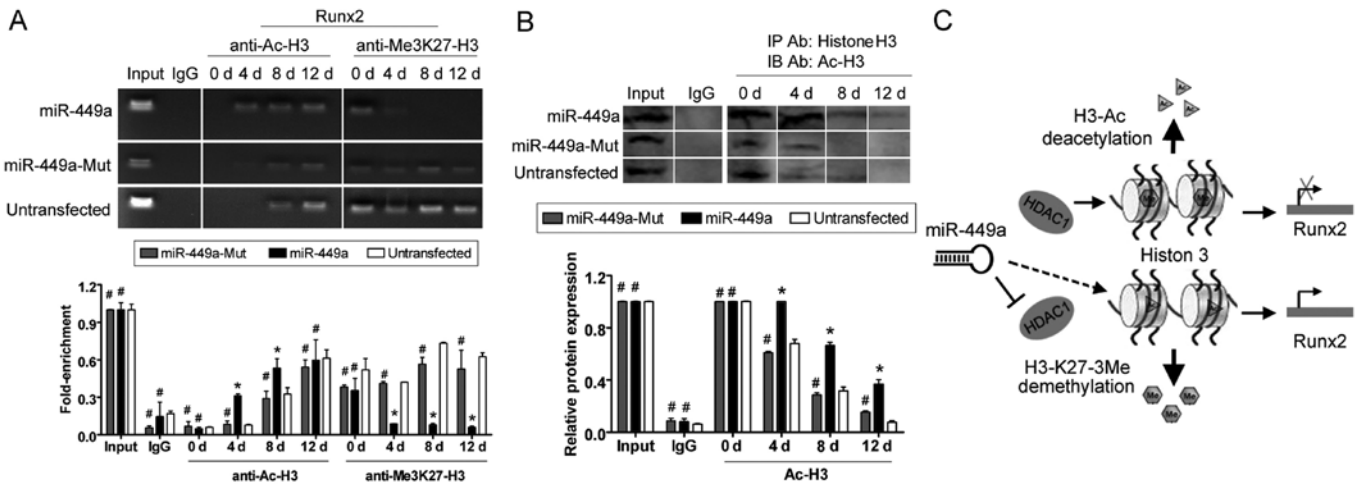
Figure 4. Histone acetylation and *Runx2* transcriptional activity. (A) Chromatin immunoprecipitation (ChIP) assays were performed to evaluate histone H3 acetylation levels in the *Runx2* promoter at each time-point after induction of differentiation. Four, eight and 12 days after induction of differentiation, histone H3 was acetylated in the *miR-449a*-transfected human-induced pluripotent (iPS) cells group, compared to the same region in the *miR*-mut-transfected iPS or untransfected groups. By contrast, histone H3K27 was methylated in the *miR*-mut-transfected iPS and untransfected groups following induction, compared to the *miR-449a*-transfected iPS group. *P<0.05, vs. untransfected group; $^#$P>0.05 vs. untransfected group; n=3. (B) The results of co-IP western blotting indicated that the level of endogenous H3Ac was maintained at a higher level in the *miR-449a*-transfected iPS group during differentiation. *P<0.05, vs. untransfected group; $^#$P>0.05, vs. untransfected group; n=3. (C) Model showing that *miR-449a* was capable of maintaining the *Runx2* locus in an active transcriptional state through silencing *HDAC1* expression and covalent histone modifications. IgG, immunoglobulin G. d, day.
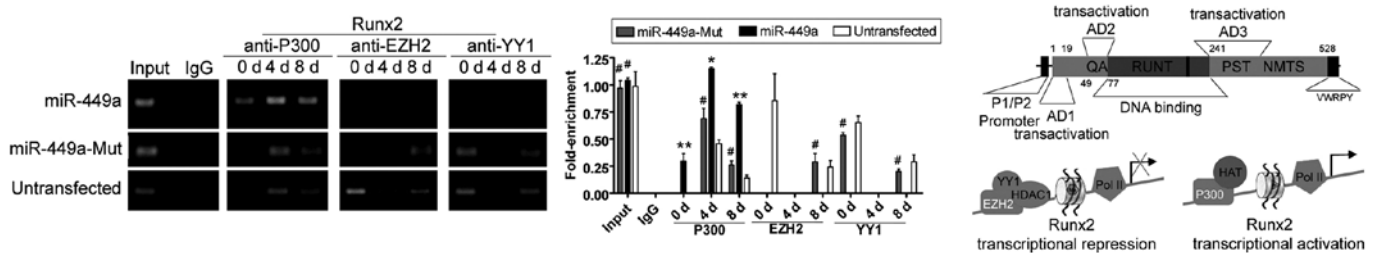

Figure 5. Chromatin re-configuration at the *Runx2* locus during osteoblast differentiation. Chromatin immunoprecipitation (ChIP) assays were performed with antibodies against P300/CBP, EZH2 and YY1 using DNA harvested from each human-induced pluripotent (iPS) cells group during 0, four and eight days after induction of differentiation. Enriched DNA fragments of the *Runx2* gene promoter from these ChIP assays were analyzed by PCR and expressed as relative fold enrichment following subtraction of the matched immunoglobulin G (IgG)-negative control. In the *miR-449a*-transfected iPS group during four and eight days after induction of differentiation, the binding efficiency of the *Runx2* gene promoter in combination with P300/CBP protein was much higher compared to the combination with EZH2 and YY1. However, the binding efficiency of the *Runx2* gene promoter in combination with EZH2 and YY1 proteins was higher compared to the combination with P300/CBP in the *miR*-mut-transfected iPS or untransfected groups during four and eight days after induction of differentiation. **P<0.01, vs. untransfected group; *P<0.05 vs. untransfected group; $^#$P>0.05 vs. untransfected group; n=3. d, day.

promoter were higher compared to the miR-mut-transfected iPS or untransfected groups (Fig. 4). However, K27 trimethylation levels of histone H3 in the *Runx2* promoter were elevated in the *miR*-mut-transfected iPS and untransfected groups, but not in the *miR-449a*-transfected iPS group following induction of differentiation. In addition, the results of western blotting indicated that the level of H3Ac was maintained at a high level in the *miR-449a*-transfected iPS group; by contrast, the expression level of H3Ac rapidly declined in the *miR*-mut-transfected iPS or untransfected groups following induction of differentiation (Fig. 4). However, in the *miR-449a*-transfected iPS group during four and eight days after induction of differentiation, the binding efficiency of the *Runx2* gene promoter in combination with the P300/CBP protein was much higher compared to the combination with EZH2 and YY1 (Fig. 5). However, in the *miR*-mut-transfected iPS or untransfected groups during four and eight days after induction of differentiation, the binding efficiency of the *Runx2* gene promoter in combination with the

EZH2 and YY1 proteins was higher compared to the combination with P300/CBP (Fig. 5).

Discussion

Osteoblast differentiation is a complex process involving the precise regulation of the activation and suppression of genes in response to physiological signals (9). At a biochemical level, the primary pathway involves bone morphogenetic protein (BMP)-Smad signaling, which leads to the activation of osteoblast-essential genes, including *Runx2* and osterix (9). Previous studies have showed that *Runx2* is highly expressed in osteoblasts and osteosarcoma cells (11-16). In our preliminary experiments, the expression level of *Runx2* increased when human iPS cells were induced to differentiate into osteoblasts, indicating that the expression of *Runx2* is involved in osteoblast differentiation. However, the mechanism for regulating the expression of *Runx2* was unclear. Although it has previously been possible to induce

iPS cells and ESCs to differentiate into osteoblasts *in vitro*, this was a long and inefficient process, requiring ~16 days to achieve mature osteoblasts (3,7-9,16). In these studies, the *Runx2* gene expression was induced but remained at a low level. In addition, our preliminary experiments showed that histone acetylation decreased during the process of iPS cell differentiation into osteoblasts, and HDAC expression increased. With regards to the knowledge that histone acetylation is closely linked with the activation of gene transcription, and that overexpression of HDAC induced histone deacetylation, it can be speculated that an increase in HDAC expression during differentiation would lead to a decrease in the transcription of *Runx2*, which would be counter-productive to osteoblast differentiation. However, the mechanism behind HDAC overexpression during the induction of differentiation into osteoblasts is not understood. The overexpression of HDAC1 was possibly due to *miR-449a* downregulation, and forced overexpression of *miR-449a* may promote osteogenesis. The experiments of the present study demonstrated that silencing of endogenous *HDAC1* expression by overexpression of *miR-449a* maintained histone acetylation levels, induced *Runx2* gene transcription and stimulated osteoblast differentiation in human iPS cells more efficiently and rapidly compared to previous studies.

By contrast, in the present study *miR-449a* improved the transcriptional activity of *Runx2* via chromatin re-configuration during osteoblast differentiation. In previous studies, chromatin conformation led to differences in gene transcription activity. A number of genes adopt a conformation that is repressive for transcription, owing to the recruitment of the Polycomb group (PcG) methyltransferase EZH2, which silences transcription by catalysing trimethylation of H3-K27 (25-27). EZH2 was recruited to the histone regulatory regions via interaction with Yin Yang 1 (YY1), and further association with HDAC1 formed a repressive complex (25-27). In addition, YY1 was a multifunctional transcription factor. Certain transcription co-repressory complexes containing nuclear HDACI and EZH2 together with YY1 were recruited to chromatin to silence transcription of the target genes. The above process suppressed the hyperacetylation of histone-specific lysines and promoted di- and tri-methylation of specific lysines (such as K9 and K27) to generate a chromatin conformation that is repressive for transcription of the target genes (28,29). YY1 also directly interacts with a number of proteins with important epigenetic modifications, including P300/CBP and HDAC1 for protein acetylation and deacetylation, and EZH2 for histone methylation. As a member of the PcG proteins, it not only directly interacted with DNA at a consensus binding site to establish and maintain gene repression, but also together with EZH2-mediated H3-K27 trimethylation, in order to mediate histone modification and chromatin remodeling (27-29). These enzymes catalyzed histone modifications, including H3-K27 trimethylation that established a chromatin conformation that is repressive for transcription. In view of the above evidence, it can be speculated that the transcriptional activity of *Runx2* was closely associated with co-repressory complexes or the transcription activator complex. The present study showed that the binding efficiency of the *Runx2* gene promoter in combination with P300/CBP protein was much higher than the combination with EZH2 and YY1 in the *miR-449a*-transfected iPS group during four and eight days after induction of

differentiation. However, the binding efficiency of the *Runx2* gene promoter in combination with EZH2 and YY1 proteins was higher compared to the combination with P300/CBP in the *miR-mut*-transfected iPS or untransfected groups during four and eight days after induction of differentiation. These results indicated that the transcription of the *Runx2* gene was activated via chromatin reconfiguration into a conformation permissive for transcription in the *miR-449a*-transfected iPS group, but not in the other two groups. Therefore, *miR-449a* improved the transcriptional activity of *Runx2* via chromatin re-configuration.

Acknowledgements

References

1. Liu T, Zou G, Gao Y, *et al*: High efficiency of reprogramming CD34(+) cells derived from human amniotic fluid into induced pluripotent stem cells with Oct4. Stem Cells Dev 21: 2322-2332, 2012.
2. Liu T, Cheng W, Huang Y, Huang Q, Jiang L and Guo L: Human amniotic epithelial cell feeder layers maintain human iPS cell pluripotency via inhibited endogenous microRNA-145 and increased Sox2 expression. Exp Cell Res 318: 424-434, 2011.
3. Jin GZ, Kim TH, Kim JH, *et al*: Bone tissue engineering of induced pluripotent stem cells cultured with macrochanneled polymer scaffold. J Biomed Mater Res A 101: 1283-1291, 2012.
4. Takahashi K and Yamanaka S: Induction of pluripotent stem cells from mouse embryonic and adult fibroblast cultures by defined factors. Cell 126: 663-676, 2006.
5. Takahashi K, Tanabe K, Ohnuki M, *et al*: Induction of pluripotent stem cells from adult human fibroblasts by defined factors. Cell 131: 861-872, 2007.
6. Kuroda S, Sumner DR and Virdi AS: Effects of TGF-beta1 and VEGF-A transgenes on the osteogenic potential of bone marrow stromal cells in vitro and in vivo. J Tissue Eng 3: 2041731412459745, 2012.
7. Diekman BO, Christoforou N, Willard VP, *et al*: Cartilage tissue engineering using differentiated and purified induced pluripotent stem cells. Proc Natl Acad Sci USA 109: 19172-19177, 2012.
8. Buttery LD, Bourne S, Xynos JD, *et al*: Differentiation of osteoblasts and in vitro bone formation from murine embryonic stem cells. Tissue Eng 7: 89-99, 2001.
9. Okamoto H, Matsumi Y, Hoshikawa Y, Takubo K, Ryoke K and Shiota G: Involvement of microRNAs in regulation of osteoblastic differentiation in mouse induced pluripotent stem cells. PLoS One 7: e43800, 2012.
10. Hou X, Shen Y, Zhang C, *et al*: A specific oligodeoxynucleotide promotes the differentiation of osteoblasts via ERK and p38 MAPK pathways. Int J Mol Sci 13: 7902-7914, 2012.
11. Zhang X, Ting K, Bessette CM, *et al*: Nell-1, a key functional mediator of *Runx2*, partially rescues calvarial defects in *Runx2*(+/-) mice. J Bone Miner Res 26: 777-791, 2010.
12. Nishimura R, Wakabayashi M, Hata K, *et al*: Osterix regulates calcification and degradation of chondrogenic matrices through matrix metalloproteinase 13 (MMP13) expression in association with transcription factor *Runx2* during endochondral ossification. J Biol Chem 287: 33179-33190, 2012.
13. Iwasaki M, Piao J, Kimura A, *et al*: *Runx2* haploinsufficiency ameliorates the development of ossification of the posterior longitudinal ligament. PLoS One 7: e43372, 2012.
14. Li X, Huang M, Zheng H, *et al*: CHIP promotes *Runx2* degradation and negatively regulates osteoblast differentiation. J Cell Biol 181: 959-972, 2008.
15. Lucero C, Vega O, Osorio M, *et al*: The cancer-related transcription factor *Runx2* modulates cell proliferation in human osteosarcoma cell lines. J Cell Physiol 228: 714-723, 2012.

16. Hu X, Zhang X, Dai L, et al: Histone deacetylase inhibitor trichostatin A promotes the osteogenic differentiation of rat adipose-derived stem cells by altering the epigenetic modifications on Runx2 promoter in a BMP signaling-dependent manner. Stem Cells Dev 22: 248-255, 2012.
17. Buurman R, Gürlevik E, Schäffer V,, et al: Histone deacetylases activate hepatocyte growth factor signaling by repressing microRNA-449 in hepatocellular carcinoma cells. Gastroenterology 143: 811-820. e811-e815, 2012.
18. Jeon HS, Lee SY, Lee EJ, et al: Combining microRNA-449a/b with a HDAC inhibitor has a synergistic effect on growth arrest in lung cancer. Lung Cancer 76: 171-176, 2011.
19. Noonan EJ, Place RF, Pookot D, et al: miR-449a targets HDAC-1 and induces growth arrest in prostate cancer. Oncogene 28: 1714-1724, 2009.
20. Liu T, Chen Q, Huang Y, Huang Q, Jiang L and Guo L: Low microRNA-199a expression in human amniotic epithelial cell feeder layers maintains human-induced pluripotent stem cell pluripotency via increased leukemia inhibitory factor expression. Acta Biochim Biophys Sin (Shanghai) 44: 197-206, 2012.
21. Cheng W, Liu T, Wan X, Gao Y and Wang H: MicroRNA-199a targets CD44 to suppress the tumorigenicity and multidrug resistance of ovarian cancer-initiating cells. FEBS J 279: 2047-2059, 2012.
22. Zhang L, Liu T, Huang Y and Liu J: microRNA-182 inhibits the proliferation and invasion of human lung adenocarcinoma cells through its effect on human cortical actin-associated protein. Int J Mol Med 28: 381-388, 2011.
23. Mukherjee A and Rotwein P: Selective signaling by Akt1 controls osteoblast differentiation and osteoblast-mediated osteoclast development. Mol Cell Biol 32: 490-500, 2011.
24. Cheng W, Liu T, Jiang F, et al: microRNA-155 regulates angiotensin II type 1 receptor expression in umbilical vein endothelial cells from severely pre-eclamptic pregnant women. Int J Mol Med 27: 393-399, 2011.
25. Guasconi V and Puri PL: Chromatin: the interface between extrinsic cues and the epigenetic regulation of muscle regeneration. Trends Cell Biol 19: 286-294, 2009.
26. Forcales SV and Puri PL: Signaling to the chromatin during skeletal myogenesis: novel targets for pharmacological modulation of gene expression. Semin Cell Dev Biol 16: 596-611, 2005.
27. Caretti G, Di Padova M, Micales B, Lyons GE and Sartorelli V: The Polycomb Ezh2 methyltransferase regulates muscle gene expression and skeletal muscle differentiation. Genes Dev 18: 2627-2638, 2004.
28. Zhang Q, Stovall DB, Inoue K and Sui G: The oncogenic role of Yin Yang 1. Crit Rev Oncog 16: 163-197, 2012.
29. Affar el B, Gay F, Shi Y, et al: Essential dosage-dependent functions of the transcription factor yin yang 1 in late embryonic development and cell cycle progression. Mol Cell Biol 26: 3565-3581, 2006.